ACKNOWLEDGMENT

We are grateful to the Apple Pollination Division of the Long Ashton Research Station for the use of the apple trees for the investigation.

Registry No. Fenitrothion, 122-14-5.

LITERATURE CITED

Bayer, D. E.; Lumb, J. M. In "Pesticide Formulations"; Van Valkenburg, W., Ed.; Marcel Dekker: New York, 1973; Chapter 9.
Becher, P. In "Pesticide Formulations"; Van Valkenburg, W., Ed.; Marcel Dekker: New York, 1973; Chapter 2.
Bowman, M. C.; Beroza, M. *J. Agric. Food Chem.* **1969**, *17*, 271–276.
Eglinton, G.; Gonzalez, A. G.; Hamilton, R. J.; Raphael, R. A. *Phytochemistry* **1962**, *1*, 89–102.
Goodman, R. W. In "Advances in Pest Control Research"; Metcalf, R. L., Ed.; Interscience: New York, 1962; Vol. V, pp 1–46.
Holly, K. In "Herbicides"; Audus, L. J., Ed.; Academic Press: London, 1976; Vol. 2, Chapter 8.
Jansen, L. L. *Weeds* **1961**, *9*, 381–405.
Leuck, D. B.; Bowman, M. C. *J. Econ. Entomol.* **1969**, *62*, 1282–1285.
Martin, J. T. *J. Sci. Food Agric.* **1960**, *11*, 635–640.
Ohkawa, H.; Mikami, M.; Miyamoto, J. *Agric. Biol. Chem.* **1974**, *38*, 2247–2255.
Price, C. E. *Spec. Publ.—Chem. Soc.* **1977**, *No. 29*, 42–66.
Roberts, M. F.; Martin, J. T.; Peries, O. S. *Annu. Rep. Long Ashton Res. Stn. 1960* **1961**, 102.
Silva Fernandes, A. M.; Baker, E. A.; Martin, J. T. *Ann. Appl. Biol.* **1964**, *53*, 43–58.

Received for review June 29, 1982. Revised manuscript received April 15, 1983. Accepted July 19, 1983.

New Perspectives on the Hydrolytic Degradation of the Organophosphorothioate Insecticide Chlorpyrifos

Donald L. Macalady[1] and N. Lee Wolfe*

The disappearance kinetics in water for chlorpyrifos [*O,O*-diethyl *O*-(3,5,6-trichloro-2-pyridyl) phosphorothioate], an important insecticide, has been investigated to provide a kinetic expression to define the hydrolysis process in aquatic ecosystems. Pseudo-first-order kinetics are observed over the pH range of 1–13. The rate constant is independent of pH from pH 1 to pH 7 and has a value of $(6.2 \pm 0.9) \times 10^{-6}$ min^{-1} at 25 °C. At alkaline pHs, the rate constant is much larger but is not directly proportional to hydroxide activity. The observed behavior over the pH range 10–12 is consistent, however, with equilibrium formation of a 5-coordinate charged hydroxyphosphorothioate intermediate and the rate-controlling decomposition of this intermediate to products. Thus, the second-order rate expression does not accurately describe the kinetics of degradation at alkaline pHs. Product studies over the alkaline pH range (9–13) show that the only major products are 3,5,6-trichloro-2-pyridinol and *O,O*-diethyl phosphorothioic acid.

Organophosphorothioates comprise a large and important class of compounds in use as environmental chemicals ("Farm Chemicals Handbook", 1981). Because these compounds may appear in environmental waters, efforts have been made to describe the chemical reactions that these compounds undergo in aquatic ecosystems (Wolfe et al., 1978; Paris et al., 1981). In particular, recent hydrolysis and biolysis studies have focused on the development of quantitative expressions for use in models to forecast the fate of such pollutants in aquatic ecosystems. These usually detailed studies are aimed at obtaining the disappearance rate constants in either first-order or second-order rate expressions.

Detailed knowledge of the kinetics of the alkaline and neutral hydrolysis pathways is critical to several areas of environmental chemistry. Such knowledge is particularly pertinent in designing experiments to obtain reliable rate constants for use in assessing the fate and transport of pollutants in aquatic ecosystems. Another example is the development of structure reactivity relationships for use in predicting alkaline or neutral hydrolysis rate constants of organophosphate and phosphorothioate esters (Wolfe, 1980). The correlation between alkaline hydrolysis and some physiochemical property of the congeners (e.g., pK_a of the leaving group) requires a data base of alkaline hydrolysis rate constants. Even more fundamental is an understanding of the microbial degradation process and the relationship between enzymatic hydrolysis and abiotic hydrolysis (Wolfe et al., 1980). Such relationships have been reported for other classes of compounds and have potential in elucidating the degradative pathways of phosphorothioate esters in the aquatic environment.

Chlorpyrifos, a model compound representative of the organophosphorothioate insecticides, was studied in aquatic ecosystems because of its potential to hydrolyze not only in the water column but also in the bottom sediments. It is generally accepted that the alkaline hydrolysis of organophosphorus esters is described by a second-order rate expression that is first order in ester and first order in hydroxide ion activities (Cox and Ramsay, 1964). Thus, a plot of log observed rate constant vs. pH for the alkaline hydrolysis should be linear with a slope of 1. In the case of chlorpyrifos, however, such a plot is nonlinear. Fur-

U.S. Environmental Protection Agency, Athens, Georgia 30613.
[1]National Research Council Senior Fellow. Present address: Department of Chemistry and Geochemistry, Colorado School of Mines, Golden, CO 80401.

0021-8561/83/1431-1139$01.50/0

thermore, detailed studies of the alkaline hydrolysis mechanism suggest that it proceeds, at least over a substantial pH range, via a two-step process. In this paper a kinetic expression, consistent with pH effects, products, ionic strengths, and solvent effects, has been derived for chlorpyrifos.

EXPERIMENTAL SECTION

Instrumental. Gas chromatographic (GC) analyses were performed using a Tracor MT 222 gas chromatograph equipped with ^{63}Ni electron capture and H_2 flame ionization detectors. For electron capture determinations, a 2 mm i.d. × 2 m long glass column packed with 10% SE-30 on 80–100-mesh Gas-Chrom Q was used. Operating conditions included injector, detector, and column oven temperatures of 215, 285, and 185–200 °C, respectively, and a N_2 carrier gas flow rate of 8 mL/min. Conditions for H_2 flame analyses are given below.

Gas chromatographic–mass spectrometric (GC–MS) analyses were achieved using a Finnigan Model 4023 GC–MS system in the EI mode at 70 eV. The GC portion contained a 30-m fused silica–SE-54 capillary column, with a programmed oven temperature from 45 to 240 °C at 8 °C/min.

LC analyses were performed using a Micromeritics Model 750 solvent delivery system with a Model 786 variable-wavelength UV detector set at 220 nm. A 5.0 mm i.d. × 300 mm long Microsil C_{18} (7.5 μm) column, with 70% CH_3CN–30% H_2O as the eluent at a constant flow of 1.5 mL/min, was used.

Liquid chromatographic–mass spectrometric (LC–MS) analyses were performed with a Waters Associates 204 liquid chromatograph coupled to a tee that split the LC effluent in a 1:1 ratio to waste and onto a Kapton belt transport Finnigan LC–MS interface. The LC utilized a Waters Model 400 dual-wavelength ultraviolet (UV) absorbance detector (254 and 280 nm) and a 2.9 mm i.d. × 30 cm long, Bondapak C_{18} column with a 90% CH_3CN–10% H_2O eluent. The Finnigan 3200 mass spectrometer was used in both the electron ionization (EI) and methane chemical ionization (CI) modes at 70 and 100 eV, respectively. The MS was interfaced to a System 150 data system.

Hydrogen ion activities below a pH of 11.5 were obtained by using a Corning Model 112 pH meter equipped with an Orion pH probe standardized with commercially prepared buffers. At pHs above 11.5, solutions were titrated with a potassium hydrogen phthalate (KHP) solution to determine hydrogen ion concentrations. Concentrations were converted to estimated activity by utilizing tabulated activity coefficients (Bates, 1964).

Chemicals. All solvents and chemicals were used as supplied from commercial sources. Chlorpyrifos, chlorpyrifos-oxon, and 3,5,6-trichloro-2-pyridinol were supplied by Dow Chemical Co. Structures were confirmed by GC–MS and proton nuclear magnetic resonance. Hydrochloric acid, sodium carbonate, sodium bicarbonate, and sodium hydroxide (used for pH adjustment) were used as commercially supplied reagent chemicals. A carbonate–bicarbonate buffer system was employed to maintain constant pH for trials between pHs of 8 and 11.

Purity checks on chlorpyrifos included melting point determination [43.0–43.2 °C observed; 42–43.5 °C literature (Brust, 1966)], electron capture GC, GC–MS, and LC–MS analyses of a millimolar solution of chlorpyrifos in 33% methanol–water solution. No significant impurities were detectable; in particular, chlorpyrifos-oxon and trichloropyridinol were present in less than 1.0 and 0.01% quantities, respectively.

For all reported kinetic runs in water, chlorpyrifos was introduced into reaction mixtures as the saturated water solution. Saturated solutions were prepared by introducing 5 mL of a concentrated (0.05 M) hexane solution into a sterile, 500-mL Erlenmeyer flask containing 100 mL of sterile 1-mm glass beads. The hexane was evaporated with a stream of N_2 gas, and the flask was filled with sterile distilled deionized water. After several days at room temperature, the solution was refrigerated for 2 or 3 days before it was filtered (cold) through 0.22-μm Nucleopore filters. The resulting solution, approximately 3×10^{-6} M chlorpyrifos, was stored at 4 °C for periods of up to 2 months before use.

Concentrations of chlorpyrifos were determined in isooctane extracts of the experimental water solutions. The isooctane contained 5×10^{-8} M hexachlorobenzene (HCB) as an internal standard. Experimental concentrations were calculated by comparing the peak height ratio for extracted chlorpyrifos to HCB with ratios in standard solutions of chlorpyrifos in 5×10^{-8} M HCB isooctane. Standard curves were generally linear ($r^2 > 0.99$) over the concentration range (0.5×10^{-8} to 1×10^{-6} M), with a minimum working concentration (in the extract) of 0.5×10^{-8} M chlorpyrifos.

In some experiments, concentration data were obtained by LC analyses of chlorpyrifos. Direct injections of 10–50% methanol–water or acetonitrile–water solutions of chlorpyrifos were used at initial concentrations between 6×10^{-5} and 6×10^{-4} M. Concentrations were calculated for each solvent system from standard curves relating LC peak heights to concentrations.

Kinetic Procedures. The process of collecting information to determine disappearance kinetics followed one of two general procedures. The first procedure, by which most concentration data were obtained, involved periodically removing aliquots from a bulk solution of chlorpyrifos in pH-adjusted or buffered distilled deionized water in a glass-stoppered flask. Aliquots were then added to a measured quantity of HCB–isooctane, the mixture was thoroughly shaken on a vortex mixer, and the isooctane layer analyzed for chlorpyrifos by GC. Careful tests for extraction efficiency and for any pH dependence in extraction efficiency were conducted to assure complete recovery of chloropyrifos. Recoveries of >95% added chlorpyrifos were considered satisfactory. A detailed description of one typical experiment follows.

Two 500-mL glass-stoppered Erlenmeyer flasks were filled with hot 6 N HCl and allowed to stand for several hours. The flasks were emptied and rinsed well with tap water, with distilled water, with acetone, with distilled water, and finally twice with distilled deionized water. After being dried in a 150 °C oven, the cooled flasks each were filled as follows. Approximately 1 L of distilled water was adjusted with 1.0 M NaOH to a pH of 11.2, and 400 mL of this was added to each of two flasks, along with 50 mL of saturated aqueous chlorpyrifos solution. The flasks were swirled to mix the contents and then placed on a flatbed shaker in a 25 °C constant temperature room. Subsequently, 2 mL of the saturated chlorpyrifos solution was added to two 10-mL aliquots of 5×10^{-8} M HCB–isooctane in 15-cm, glass-stoppered test tubes. The tubes were vortex mixed for at least 30 s and placed in a refrigerator for future analyses and calculation of initial chlorpyrifos concentration.

After 1 h, 2-mL aliquots were withdrawn from each of the Erlenmeyer flasks and added to 5 mL of 5×10^{-8} M HCB–isooctane in 15-cm, glass-stoppered test tubes. The tubes were vortex mixed for 30 s and placed in a refrig-

erator (4 °C) to allow components to separate before analysis. Also withdrawn at this time were 25-mL aliquots for immediate pH determination. The flasks were not agitated for the remainder of the study. Aliquots were subsequently withdrawn from the flasks at times 120, 390, 900, 1470, 1800, 2400, and 2700 min from initial mixing with chlorpyrifos.

At t = 2700 min, the contents were emptied as completely as possible (by shaking) from each of the flasks in order to determine the amount of chlorpyrifos sorbed to the vessel walls. The volume and final pH of the solutions were also determined at this time.

To each of the 500-mL flasks was added 50 mL of CH_3CN. This was swirled around to thoroughly wet the container walls; 150 mL of distilled deionized water and 10 mL of 5×10^{-8}, M HCB–isooctane were added. The flasks were placed in a sonicating water bath for 30 min with thorough shaking at 2-min intervals. The isooctane layer was subsequently isolated and analyzed by GC for chlorpyrifos that had been sorbed to the walls of the flasks. (In flasks prewashed as described above, the fraction of total remaining chlorpyrifos that was sorbed to the walls ranged from 0.13 to 0.005, with most values <0.020.)

The isooctane extracts from the time course samples were analyzed, at least in duplicate, by GC (electron capture), and the concentration of chlorpyrifos remaining at each time, t, was calculated from a standard plot of peak height ratios vs. concentration. The standard curve was generated from data obtained on the same day as the analyses. Pseudo-first-order rate constants, k_{obsd}, for the duplicate trials were calculated via a least-squares analysis of natural log concentration vs. time data by using a computer program written for the Hewlett-Packard 41C hand calculator.

All rate determinations were made using procedures similar to the above. Values for k_{obsd} were corrected for sorption to the walls of the flasks if sorption was significant (>2% of total chlorpyrifos). Correction was made by dividing the calculated k_{obsd} by the fraction in solution, which gives a corrected k_{obsd} if it is assumed that the sorption–desorption process is faster than hydrolysis. Values for k_{obsd} calculated from duplicate trials at pHs above 9.5 always deviated less than 10% from the average of the two values.

In addition, alkaline hydrolysis was investigated by using a second procedure at a variety of pHs in methanol–water and acetonitrile–water solutions at considerably higher initial concentrations. This enabled direct injection of the reaction mixtures on the LC–MS and LC systems for product analyses and kinetic information. Standard solutions of chlorpyrifos, 3,5,6-trichloro-2-pyridinol, triethyl thiophosphate, and partially hydrolyzed triethyl thiophosphate in methanol–water were also analyzed by direct injection into the LC–MS system.

Biodegradation Studies. Experiments were conducted to determine whether biodegradation was a significant factor in our experiments with chlorpyrifos. More than 20 degradation experiments were run with ambient (10^5–10^7 cells/L) and enriched (up to 10^{11} cells/L) populations of naturally occurring (in North Georgia lakes, ponds and streams) microorganisms. These experiments were based on previously published procedures (Paris et al., 1981).

Product Studies. Products from the alkaline hydrolysis reactions were identified by several methods. From the aqueous studies, final reaction solutions were acidified to pH 2 and freeze-dried. The residues were subsequently redissolved in 2 or 3 mL of acetonitrile, achieving a concentration factor of about 100 over the initial aqueous solutions. The acetonitrile solutions were analyzed by LC–MS and in one case by GC–MS.

The methanol–water solutions were analyzed by direct injection into the LC–MS, as were all of the acetonitrile–water reaction solutions. These mixed solvent solutions were analyzed at several times during the course of the reactions at various pHs rather than only near the completion of the reactions as was the case for the reactions in water. In addition, reaction solutions in 25% CH_3CN–water at pHs of 11.4 and 12.4 were acidified to pH 2 after 3 days of reaction time, and ca. 100 mL of each reaction mixture was freeze-dried. The freeze-dried residues were redissolved in a few milliliters of diethyl ether and methylated with diazomethane (Webb et al., 1973). The ether solution of methylated reaction products was examined by GC–MS and LC–MS.

Analyses were designed to identify the nature of the reaction products from the room temperature neutral hydrolysis reaction. Direct determination, however, was hampered by three factors. One was the extremely low concentrations of chlorpyrifos used. Such concentrations were used because of our desire to conduct experiments at environmentally relevant concentrations and because of the low solubility of chlorpyrifos (4.1×10^{-6} M) at room temperature. A second was the high water solubility of the expected reaction products. Even at acid pHs, products such as trichloropyridinol and diethyl thiophosphoric acid are not extractable into organic solvents. A third was the slow rate of the reaction. Accumulation of quantities of reaction products detectable by LC or MS analysis, even with a replenishing supply of chlorpyrifos, would take many months.

Consequently, our attempts were limited to efforts to identify reaction products from the neutral hydrolysis at elevated temperatures (70–80 °C). Chlorpyrifos-coated glass beads were added to chlorpyrifos-saturated water in a sealed 1-L vessel. The vessel was maintained at 80 °C for 20 h, after which it was removed and cooled in an ice bath. Two 5-mL aliquots were withdrawn for analyses, and the vessel was resealed and returned to the 80 °C bath. After 7 additional h, two 5.0-mL aliquots were withdrawn from the hot vessel for extraction and chlorpyrifos analysis by electron capture GC. Presumably any volatile reaction products (such as ethanol) escaped while the vessel was open. This entire procedure with the vessel sealed was then repeated after an additional 15 h at 80 °C. The pH of the sampled solutions was also determined at this time.

Finally, the sealed vessel was held at 70 °C for an additional 65 h. The vessel and its contents were then cooled to 0 °C, and three 5-mL aliquots were removed. The entire solution was decanted from the glass beads (volume 100 mL) into a beaker, and the pH was determined prior to adjustment to pH 2 with concentrated HCl. The solution was freeze-dried after which the residue was redissolved in 5 mL of diethyl ether and methylated with diazomethane.

The methylated, nonvolatile reaction products were analyzed by GC–MS. One sample from each set of duplicated aliquots that were removed from the cooled reaction mixture during the course of the reaction was analyzed for ethanol by direct injection into a GC equipped with a 3-ft glass column packed with Porapak QS (50–80 mesh) and with a hydrogen flame ionization detector. The column oven temperature was 120 °C. The minimum quantifiable concentration was 2 mg of ethanol/L. The other of the duplicate samples was analyzed by LC–MS for additional reaction products. The aliquots removed

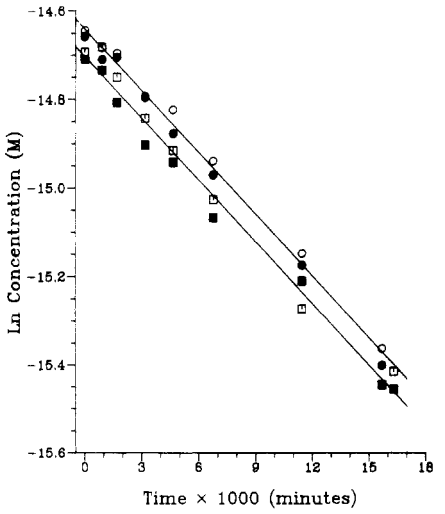

Figure 1. Plot of ln concentration (M) vs. time for the hydrolysis of chlorpyrifos at pH 9.7 with two different carbonate buffer concentrations. Open and closed circles: two runs at 0.05 M buffer. Open and closed squares: two runs at 0.0012 M buffer (T = 25 °C).

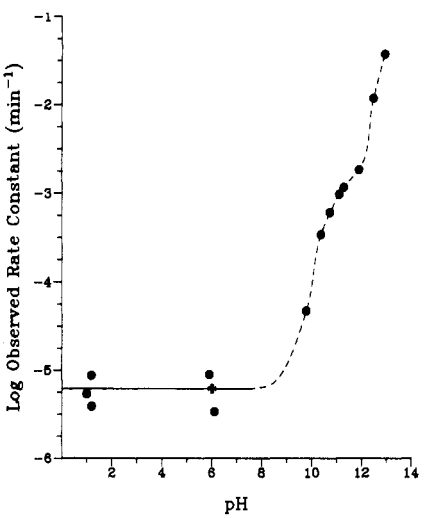

Figure 2. Plot of log observed rate constant (min^{-1}) vs. pH for the hydrolysis of chlorpyrifos at 25 °C in buffered distilled water. Data from Table I. The cross and solid line represent the predicted neutral hydrolysis behavior.

from the reaction solution at 80 °C were analyzed for chlorpyrifos as described above.

RESULTS

First- (or pseudo-first-) order disappearance rate constants measured for chlorpyrifos in pH-adjusted distilled water are listed in Table I along with other parameters associated with each determination. The initial concentrations given are predicted values based on initial volumes of added saturated chlorpyrifos solution. These values generally agree (5%) with values calculated from the intercepts of the kinetic plots. Disagreement between predicted and calculated initial concentration occurred in several experiments where significant (>10%) sorption to container walls created an initial curvature in the kinetic plots.

Tabulated values of k_{obsd} have been corrected, where necessary, for sorption to container walls, generally by assuming the sorption–desorption reactions are fast relative to hydrolysis. In three experiments (identified in the first column of Table I), sorption and hydrolysis rates were similar enough to necessitate an alternate calculation method. For these runs, a computer fit of the experimental data to the relevant kinetic differential equations was used to calculate the rate constants.

The results of the biodegradation studies show little or no influence by microorganisms on the rate of degradation of chlorpyrifos in natural water samples. In all but two trials, degradation rates were the same within experimental uncertainty for both sterile controls and test solutions with active microorganisms. (Microorganisms were enumerated by standard dilution plate count techniques.)

In the two exceptions, significant biodegradation began only after 3 or 4 days. In these trials only, the chlorpyrifos had been introduced as an acetonitrile solution, making the test mixture approximately millimolar in CH_3CN. Because cell populations rose significantly (by × 10) during these trials, it is apparent that some naturally occurring organism that grows well on acetonitrile can also mediate the degradation of chlorpyrifos.

Catalysis by buffers was also considered, and the results of one experiment that verifies the absence of a measurable buffer catalysis is shown in Figure 1. The graph shows data from two runs at a buffer concentration of 0.05 M (carbonate–bicarbonate) and two at a lower buffer concentration of 0.0012 M. The slopes from both sets of points

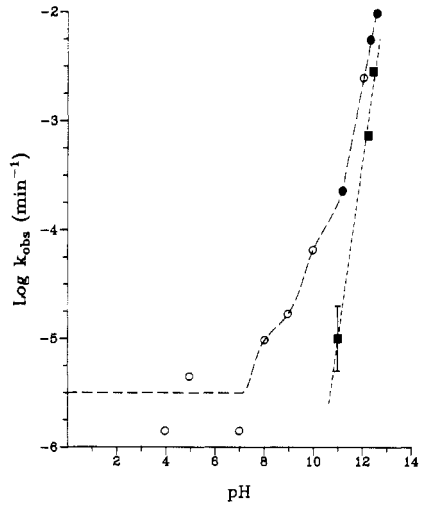

Figure 3. Plot of log observed rate constant (min^{-1}) vs. pH for the hydrolysis of chlorpyrifos at 25 °C in 50% methanol–water solutions (circles) and 50% acetonitrile–water solutions (squares). Data from Tables II and III (open circles).

are identical within experimental uncertainty (data for individual runs shown in Table I).

Figure 1 also serves to illustate a typical experimental plot. Those at higher pHs generally showed less scatter about the least-squares line: those at lower pHs usually had larger estimates of standard error.

Rate constants for the disappearance kinetics of chlorpyrifos from methanol–water and acetonitrile–water solutions are listed in Table II, along with associated experimental conditions for each run. The initial concentrations for these trials were about 2 orders of magnitude higher than for the distilled water trials.

Rate constants reported by several other investigators for the disappearance of chlorpyrifos are tabulated with other available data in Table III.

Values of the rate constants at 25 °C from our distilled water studies are illustrated via a log k_{obsd} vs. pH plot in Figure 2. A similar plot for the more limited data at 25 °C in 50% methanol–water and 50% acetonitrile–water is shown in Figure 3, which also includes some literature data from Table III. The dotted line from pH 1 to pH 7 in Figure 3 was drawn based on an estimated value for the neutral hydrolysis rate constant equal to half the distilled

Table I. Observed First-Order or Pseudo-First-Order Disappearance Rate Constants for Chlorpyrifos from Distilled or Buffered Distilled Water

	pH ± SD	temp, °C	initial concn, M	no. of kinetic points	duration of run, min	k_{obsd}, min^{-1} [c]	comments
1	1.00 ± 0.05	25.0 ± 0.1	5.0×10^{-7}	10	45 000	$(5.4 \pm 1.3) \times 10^{-6}$	
2	1.20 ± 0.05	25.0 ± 0.1	2.2×10^{-7}	10	20 000	$(3.9 \pm 1.4) \times 10^{-6}$	
3	1.20 ± 0.05	25.0 ± 0.1	2.2×10^{-7}	10	20 000	$(8.8 \pm 1.9) \times 10^{-6}$	
4	5.90 ± 0.05	25.0 ± 0.1	2.0×10^{-7}	10	30 000	$(9.0 \pm 2.1) \times 10^{-6}$	sterile
5	6.11 ± 0.05	25.0 ± 0.1	2.0×10^{-7}	10	30 000	$(3.4 \pm 1.7) \times 10^{-6}$	sterile
6	5.5 ± 0.01	35.0 ± 0.1	3.2×10^{-7}	18	40 000	$(2.2 \pm 0.2) \times 10^{-5}$	sterile
7	5.5 ± 0.01	35.0 ± 0.1	3.2×10^{-7}	18	40 000	$(2.4 \pm 0.2) \times 10^{-5}$	sterile
8	5.5 ± 0.01	35.0 ± 0.1	3.2×10^{-7}	18	40 000	$(1.4 \pm 0.3) \times 10^{-5}$	sterile
9	5.5 ± 0.01	35.0 ± 0.1	3.2×10^{-7}	18	40 000	$(2.1 \pm 0.4) \times 10^{-5}$	sterile
10	4.6 ± 0.1	45.0 ± 0.1	4.0×10^{-7}	22	11 000	$(6.77 \pm 0.17) \times 10^{-5}$	11 sets of duplicate points
11	6.02 ± 0.05	45.0 ± 0.1	1.4×10^{-7}	12	13 500	$(6.21 \pm 0.16) \times 10^{-5}$	
12	8.71 ± 0.05	45.0 ± 0.1	1.4×10^{-7}	12	13 500	$(1.15 \pm 0.03) \times 10^{-4}$	buffered, 10^{-4} M
13	6.40 ± 0.05	55.0 ± 0.1	1.35×10^{-7}	14	18 500	$(1.68 \pm 0.05) \times 10^{-4}$	
14	8.42 ± 0.05	55.0 ± 0.1	1.35×10^{-7}	14	18 500	$(2.3 \pm 0.1) \times 10^{-4}$	buffered, 10^{-3} M
15	7.35 ± 0.08	65.0 ± 0.1	1.0×10^{-7}	12	3 500	$(5.1 \pm 0.01) \times 10^{-4}$	
16	7.81 ± 0.08	65.0 ± 0.1	1.2×10^{-7}	12	3 500	$(5.2 \pm 0.01) \times 10^{-4}$	buffered, 10^{-4} M
17	9.77 ± 0.02	25.0 ± 0.1	4.4×10^{-7}	8	15 000	$(4.74 \pm 0.14) \times 10^{-5}$	high buffer, 0.05 M
18	9.77 ± 0.02	25.0 ± 0.1	4.4×10^{-7}	8	15 000	$(4.71 \pm 0.09) \times 10^{-5}$	high buffer, 0.05 M
19	9.7 ± 0.1	25.0 ± 0.1	4.1×10^{-7}	8	15 000	$(4.57 \pm 0.16) \times 10^{-5}$	low buffer, 0.0012 M
20	9.7 ± 0.1	25.0 ± 0.1	4.1×10^{-7}	8	15 000	$(4.83 \pm 0.3) \times 10^{-5}$	low buffer, 0.0012 M
21	10.34 ± 0.04[a]	25.0 ± 0.1	7.5×10^{-8}	11	7 800	$(3.03 \pm 0.21) \times 10^{-4}$	buffer, 0.008 M, sterile
22	10.37 ± 0.05[a]	25.0 ± 0.1	7.3×10^{-8}	9	7 400	$(3.50 \pm 0.17) \times 10^{-4}$	buffer, 0.008 M, sterile
23	10.35 ± 0.04	25.0 ± 0.1	8.8×10^{-8}	9	7 200	$(3.09 \pm 0.05) \times 10^{-4}$	buffer, 0.018 M, sterile
24	10.7 ± 0.1[a]	25.0 ± 0.1	3.1×10^{-8}	9	5 700	$(6.08 \pm 0.10) \times 10^{-4}$	buffer, 0.04 M, sterile
25	11.08 ± 0.1	25.0 ± 0.1	4.3×10^{-7}	9	2 650	$(1.01 \pm 0.25) \times 10^{-3}$	no buffer
26	11.05 ± 0.1	25.0 ± 0.1	5.1×10^{-7}	9	2 650	$(9.41 \pm 0.9) \times 10^{-4}$	no buffer
27	11.24 ± 0.02	25.0 ± 0.1	4.2×10^{-7}	7	2 650	$(1.08 \pm 0.07) \times 10^{-3}$	no buffer
28	11.25 ± 0.02	25.0 ± 0.1	4.9×10^{-7}	7	2 050	$(1.25 \pm 0.07) \times 10^{-3}$	no buffer
29	11.25 ± 0.03	40.0 ± 0.1	3.25×10^{-7}	7	1 200	$(4.12 \pm 0.57) \times 10^{-3}$	no buffer
30	11.25 ± 0.03	40.0 ± 0.1	3.25×10^{-7}	7	1 200	$(4.16 \pm 0.55) \times 10^{-3}$	no buffer
31	11.23 ± 0.03	50.0 ± 0.1	2.75×10^{-7}	7	570	$(5.8 \pm 0.4) \times 10^{-3}$	no buffer
32	11.23 ± 0.03	50.0 ± 0.1	2.75×10^{-7}	7	570	$(5.9 \pm 0.4) \times 10^{-3}$	titrate pH[b]
33	11.86 ± 0.01	25.0 ± 0.1	1.5×10^{-7}	7	2 140	$(1.75 \pm 0.08) \times 10^{-3}$	titrate pH[b]
34	11.86 ± 0.01	25.0 ± 0.1	1.3×10^{-7}	6	1 700	$(1.96 \pm 0.12) \times 10^{-3}$	titrate pH[b]
35	12.45 ± 0.05	25 ± 1	2×10^{-7}	5	190	$(1.19 \pm 0.03) \times 10^{-2}$	titrate pH[b]
36	12.45 ± 0.05	25 ± 1	2×10^{-7}	5	190	$(1.20 \pm 0.03) \times 10^{-2}$	titrate pH[b]
37	12.90 ± 0.05	25 ± 1	1.2×10^{-7}	5	80	$(3.78 \pm 0.08) \times 10^{-2}$	titrate pH[b]
38	12.90 ± 0.05	25 ± 1	1.2×10^{-7}	5	80	$(3.81 \pm 0.15) \times 10^{-2}$	titrate pH[b]

[a] See the text. [b] Corrected for nonunity activity coefficient. [c] Uncertainties represent the standard error in the slope of the linear least-squares fit of plots of ln concentration vs. time.

Table II. Observed Pseudo-First-Order Disappearance Rate Constants for Chlorpyrifos in Methanol-Water and Acetonitrile-Water Solutions

pH ± SD	temp, °C	initial chlorpyrifos concn, M	organic solvent	duration or run, min	k_{obsd}, min^{-1}
11.40 ± 0.05	25 ± 2	2.7×10^{-5}	12.5% CH_3OH	1 500	$(1.05 \pm 0.07) \times 10^{-3}$
12.35 ± 0.08	25 ± 2	1.5×10^{-5}	16.5% CH_3OH	240	$(9.83 \pm 0.46) \times 10^{-3}$
11.15 ± 0.05	25 ± 2	2.8×10^{-5}	25% CH_3OH	1 500	$(5.66 \pm 0.52) \times 10^{-4}$
11.15 ± 0.05	25 ± 2	4.3×10^{-5}	50% CH_3OH	3 000	$(2.31 \pm 0.11) \times 10^{-4}$
12.28 ± 0.08	25 ± 2	2.0×10^{-5}	50% CH_3OH	325	$(5.6 \pm 0.3) \times 10^{-3}$
12.53 ± 0.08	25 ± 2	5.6×10^{-4}	50% CH_3OH	325	$(9.79 \pm 0.19) \times 10^{-3}$
11.15 ± 0.05	25 ± 2	2.6×10^{-5}	12% CH_3CN	13 000	$(2.69 \pm 0.06) \times 10^{-4}$
10.96 ± 0.05	25 ± 2	2.6×10^{-5}	25% CH_3CN	13 000	$(8.13 \pm 0.42) \times 10^{-5}$
10.89 ± 0.05	25 ± 2	5.6×10^{-5}	25% CH_3CN	14 500	$(6.79 \pm 0.48) \times 10^{-5}$
10.97 ± 0.05	25 ± 2	2.6×10^{-5}	50% CH_3CN	20 000	1×10^{-5} [a]
12.2 ± 0.1	25 ± 2	7.5×10^{-5}	50% CH_3CN	2 000	$(7.41 \pm 0.28) \times 10^{-4}$
12.4 ± 0.2	25 ± 2	7.5×10^{-5}	50% CH_3CN	500	$(2.90 \pm 0.16) \times 10^{-3}$

[a] Rate constant is only approximate due to small fraction reacted during the duration of the run. Statistics on least-squares plot: $r^2 = 0.48$; slope = $-(1 \pm 0.5) \times 10^{-5}$.

water value. The activity of H_2O in 50% CH_3OH–H_2O is approximately half the pure water activity.

Experimental uncertainties are sufficiently low so as to leave little doubt that the curvatures shown in the alkaline region of these figures is not an artifact. This curvature is discussed in detail below.

Comparison of Tables I and II and Figures 2 and 3 reveals a significant solvent effect on the rate constants that is contrary to expectations for second-order alkaline hydrolysis of phosphate esters (Barnard et al., 1961). This solvent effect is also discussed below.

Rate constants measured at room temperature at pHs below 8 show considerable variation, presumably due for the most part to the difficulties inherent in measuring rate constants for very slow reactions. The absence of a pH dependence in the rate constant is obvious, however.

Table III. Literature Values for First-Order or Pseudo-First-Order Disappearance Rate Constants for Chlorpyrifos in Buffered Distilled Water or Methanol-Water Solutions

pH	temp, °C	initial concn, M	k_{obsd}, min^{-1}	comments
3.97	23		1.4×10^{-6}	50% CH_3OH-H_2O, *a*
4.7	15	3.4×10^{-7}	2.3×10^{-6}	*b*
4.7	25	3.4×10^{-7}	7.71×10^{-6}	*b*
4.7	35	3.4×10^{-7}	3.05×10^{-5}	*b*
4.95	23		4.5×10^{-6}	50% CH_3OH-H_2O, *a*
6.00	23		2.5×10^{-7}	50% CH_3OH-H_2O, *a*
	23		1.4×10^{-6}	50% CH_3OH, unbuffered, *a*
6.90	15	3.4×10^{-7}	4.9×10^{-6}	*b*
6.90	25	3.4×10^{-7}	1.4×10^{-5}	*b*
6.90	35	3.4×10^{-7}	4.2×10^{-5}	*b*
7.4	20	1×10^{-6}	9.1×10^{-6}	*c*
7.4	25		1.3×10^{-5}	calculated, *c*
7.4	37.5	1×10^{-6}	3.6×10^{-5}	*c*
8.00	23		9.7×10^{-6}	50% CH_3OH-H_2O, *a*
8.1	15	3.4×10^{-7}	8.9×10^{-6}	*b*
8.1	25	3.4×10^{-7}	2.1×10^{-5}	*b*
8.1	35	3.4×10^{-7}	1.1×10^{-4}	*b*
8.95	23		1.7×10^{-5}	50% CH_3OH-H_2O, *a*
9.96	23		6.6×10^{-5}	50% CH_3OH-H_2O, *a*
12.0	23		2.54×10^{-3}	50% CH_3OH-H_2O, *a*

[a] Brust (1966); no experimental details given. [b] Meikle and Youngson (1978); no wall effects investigated. [c] Freed et al. (1979); no wall effects investigated.

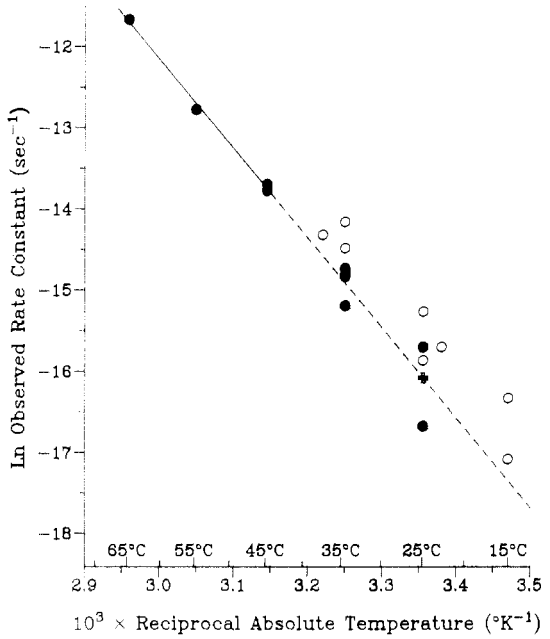

Figure 4. Arrhenius plots of ln observed rate constant (s^{-1}) vs. reciprocal absolute temperature (K^{-1}) for chlorpyrifos at neutral pHs (4.5–7.5). Data from Tables I (closed circles) and III (open circles). The cross represents an extrapolated 25 °C value (see the text).

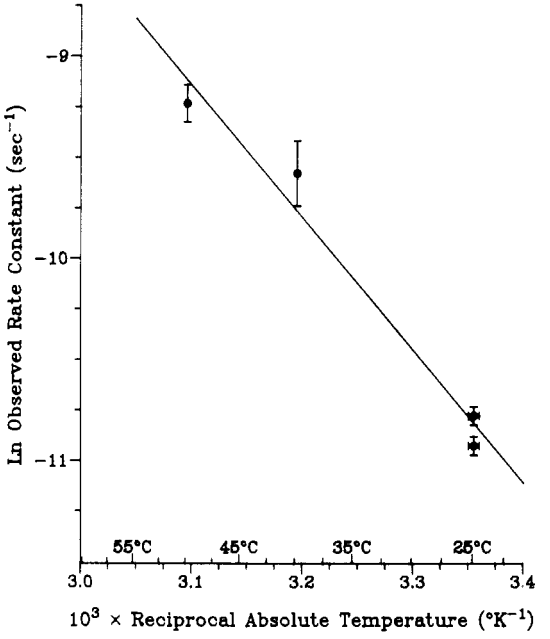

Figure 5. Arrhenius plot of ln observed rate constant (s^{-1}) vs. reciprocal absolute temperature (K^{-1}) for chlorpyrifos at a pH of 11.25. Data from Table I. Extensions of points represent experimental uncertainties.

To obtain a more accurate value for the neutral hydrolysis rate constant at lower temperatures, rate constants were determined at elevated temperatures. An Arrhenius plot [ln k vs. $1/T$ (K)] for neutral (pH 4.5–7.5) hydrolysis results is shown in Figure 4. Use of the more precise data from 65, 55, and 45 °C runs to calculate a least-squares straight line enables extrapolation to lower temperatures, resulting in more precise rate constant estimates. The accuracy of this extrapolation is supported by the agreement between the average of measured values at 35 and 25 °C and the extrapolated values: (2.04 vs. 2.03) × 10^{-5} min^{-1} at 35 °C; (6.22 vs. 6.2) × 10^{-6} min^{-1} at 25 °C. The value of 6.22 × 10^{-6} min^{-1} at 25 °C is thus our "best" value of the neutral hydrolysis rate constant for chlorpyrifos, valid over the pH range 1–7.5 at 25 °C.

The energy and entropy of activation for the neutral hydrolysis reaction can also be calculated from Figure 4 (Bunnett, 1961). The activation energy, from the slope of the Arrhenius plot, is 22.1 ± 0.8 kcal mol^{-1}, and the entropy of activation is −18 ± 3 eu at 25 °C.

Figure 5 is an Arrhenius plot for a pH of 11.25. The activation energy and entropy for the pseudo-first-order reaction at 25 °C at this alkaline pH are 13.0 ± 1.5 kcal mol^{-1} and −38 ± 5 eu. The alkaline activation energy is much lower than the neutral value, which is not unexpected based on literature values for phosphate esters (Cox and Ramsay, 1964).

The conclusion from the study of the products from the alkaline hydrolysis reaction of chlorpyrifos at pHs from 9.7 to 12.9 is that only two major products are formed: 3,5,6-trichloropyridinol and *O,O*-diethyl phosphorothioic acid. With the exception of minor amounts of *O*-methyl *O,O*-diethyl phosphorothioate in methanol–water solutions at pHs above 11, no other products were identified by LC–MS techniques. This is despite extensive searching

(using both electron and CH_4 chemical ionization modes) for any other likely, or even unlikely, products. Spectra of 3,5,6 trichloro-2-pyridinol, chlorpyrifos, chlorpyrifos-oxon, triethyl thiophosphate, and triethyl phosphate were also obtained by using the same LC–MS techniques as were used for the reaction products. These spectra were used for verification of products and for comparative purposes.

The GC–MS results for the methylated freeze-dried reaction products led to a similar conclusion. These analyses, more sensitive by 1 order of magnitude than LC–MS, showed only the methylated trichloropyridinol and methylated diethyl phosphorothioic acid plus much smaller quantities (ca. 1–5%) of methylated *O,O*-diethyl phosphoric acid, the oxygen analogue of one of the principal products. Presumably, such oxygenated forms were produced as minor byproducts as little chlorpyrifos-oxon (<1%) was detectable in the chlorpyrifos starting material.

Reaction products were also identified from the aqueous neutral hydrolysis reaction at 70–80 °C. In solutions maintained at $(2.5 \pm 0.3) \times 10^{-5}$ M chlorpyrifos for 15–20 h at 80 °C and 63 h at 70 °C, ethanol was present at levels of 4–5 mg/L, which would make ethanol a major reaction product. These levels are, however, so close to the limit of detection as to preclude further quantification. Our LC–MS procedures proved unable to detect additional reaction products in these solutions.

GC–MS analysis of the methylated nonvolatile (at pH 2) reaction products from this neutral reaction showed *O*-ethyl *O*-(3,5,6-trichloro-2-pyridyl) phosphorothioic acid to be the principle nonvolatile reaction product. Because the pH of the reaction mixture was 7.68, smaller quantities of 3,5,6-trichloro-2-pyridinol and *O,O*-diethyl phosphorothioic acid, products typical of the alkaline hydrolysis reaction, were also present.

DISCUSSION

Neutral Hydrolysis. On the basis of previous literature reports, it was anticipated that chlorpyrifos would react by a neutral hydrolysis reaction at pHs below 8 (Meikle and Youngson, 1978; Smith et al., 1978; Weber, 1976). The neutral hydrolysis rate constants, given in Table I along with the pH rate profile in Figure 2, support this pH-independent pathway over the pH range of 1–7.5. The overall reaction for the pH-independent hydrolysis is shown in eq 1. The mechanism is believed to involve

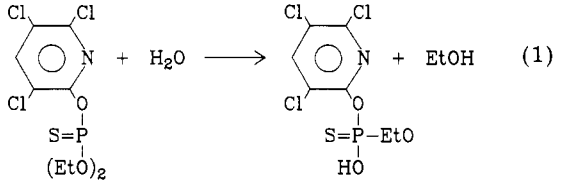

(1)

neucleophilic attack of water at the carbon of the ethoxy groups to give ethanol and *O*-(3,5,6-pyridyl) *O*-ethyl phosphorothioic acid as the products (Meikle and Youngson, 1978). The energy of activation, E_a, of 22.1 kcal mol^{-1} is similar to the values found by Meikle and Youngson (1978) and to the value of 23.4 kcal mol^{-1} reported for the neutral hydrolysis of methyl parathion (Smith et al., 1978). The average value of the rate constant $(6.2 \pm 0.9) \times 10^{-6}$ min^{-1} gives a hydrolytic half-life of 80 days at 25 °C. Similar studies of the degradation of chlorpyrifos in sediment–water samples also give a similar value for the neutral hydrolysis rate constant (Macalady and Wolfe, 1983).

Alkaline Hydrolysis. In environmental studies of the hydrolysis of organophosphate and organophosphorothioate esters, it is generally assumed that alkaline hydrolysis proceeds by simple second-order kinetics, i.e., first order in hydroxide and first order in phosphate concentration as shown in eq 2. This assumption has the advantage that, if one determines the second-order disappearance rate constant (k_2) at one alkaline pH (generally somewhere between pH 8 and pH 12), it is possible to calculate the pseudo-first-order rate constant (k_{obsd}) at any other alkaline pH (eq 3).

$$-\frac{d[P]}{dt} = k_2[P][OH^-] \quad (2)$$

$$k_{obsd} = k_2[OH^-] \quad (3)$$

Our data support the assumption that the disappearance rate constant of chlorpyrifos is first order in chlorpyrifos. On the other hand, our data do not support the assumption that the disappearance expression is first order in hydroxide activity. This is consistent with a similar conclusion reached by Brust (1966) based on studies in 50% methanol–water solutions.

Additional studies of the alkaline hydrolysis reaction were conducted to determine whether this non-second-order behavior was caused by general acid–base catalysis (GABC) or ionic strength effects resulting from pH adjustments. The data for carbonate buffered pH 9.7 (Figure 1) support the fact that GABC does not make a significant contribution to the reaction. As shown in Table I, similar results were observed at pH 10.35. Furthermore, calculations by Perdue and Wolfe (1983) suggest that at the buffer concentrations used here, buffer catalysis would be negligible. Neither are ionic strength (electrostatic) effects believed to be the cause of the deviation from first order since one of the reacting species is uncharged (Frost and Pearson, 1961).

A visual inspection of the alkaline region of the pH rate profile (Figure 2) suggests that the reaction is not first order in hydroxide activity. Linear least-squares analysis of the data from pH 9.80 to pH 13.0 gives an r^2 of 0.97; however, the slope is 0.85 ± 0.04. This deviation from 1 is not consistent with the mechanisms generally proposed for organophosphate triester hydrolysis (Barnard et al., 1961). Another way of considering the data that shows the inadequacy of the simple second-order model is to calculate values of the second-order rate "constants", k_2, from our data. Depending on the pH (between 10 and 12) selected, values of k_2 from 0.25 to 1.5 M^{-1} min^{-1} could be inferred, thus giving a factor of 6 variation in the pseudo-first-order rate constant.

Equation 4 represents a generalized reaction scheme that

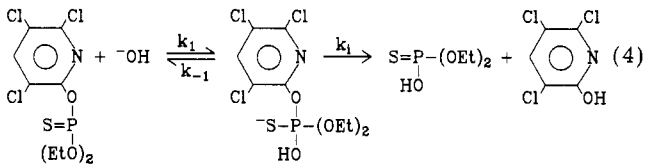

(4)

parallels the one proposed by Barnard et al. (1961) for organophosphates. In the case of organophosphate triesters, the observed second-order kinetics necessitates that $k_i \gg k_{-1}$; thus, k_1 and the OH^- activity are rate determining [see also Cox and Ramsey (1964) and Younas (1972)].

To account for the chlorpyrifos hydrolysis data, a less restrictive consideration was given to eq 4. A general expression for the value of k_{obsd} as a function of hydroxide activity implied by this mechanism is not practical because the concentration of the pentavalent charged intermediate is unknown. One can solve, however, for the value of k_{obsd} vs. OH^- activity if equilibrium in the first reaction is as-

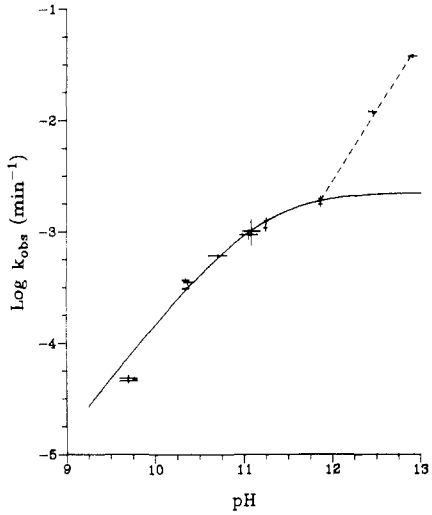

Figure 6. Plot of log observed rate constant (min^{-1}) in buffered distilled water vs. pH based on eq 6 (solid line). See the text for details. Crosses are experimental points, with uncertainties represented by the lengths of the cross axes. The dotted line is a linear least-squares fit of data at pHs of 11.86 and above. Data from Table I.

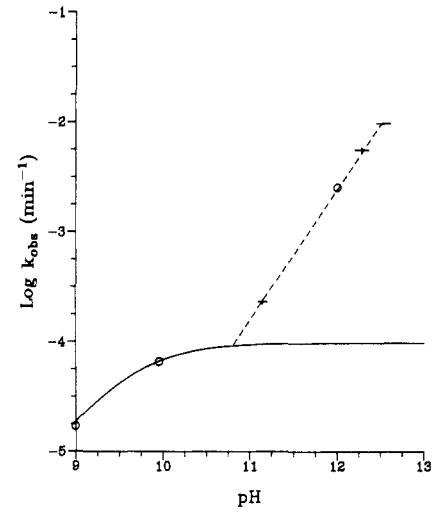

Figure 7. Plot of log observed rate constant (min^{-1}) in 50% methanol–water solutions vs. pH. The solid line represents predicted behavior based on eq 6 and experimental data at pH 9 and 10. The dashed line is a least-squares fit of data above pH 11. Data from Tables I (crosses) and III (open circles).

sumed. Defining $K = k_1/k_{-1}$, the rate expression becomes (neglecting the neutral hydrolysis contribution)

$$-\frac{d[P_T]}{dt} = \frac{k_i K[OH][P_T]}{1 + K[OH^-]} \quad (5)$$

where $[P_T]$ represents the total chlorpyrifos concentration, which includes the pentavalent intermediate. The observed first-order rate constant, consequently, is given by

$$\frac{1}{k_{obsd}} = \frac{1}{k_i} + \frac{1}{k_i K[OH^-]} \quad (6)$$

where $[OH^-]$ here represents hydroxide *activity*.

Equation 6 implies that, under conditions where equilibrium between chlorpyrifos and the charged intermediate is maintained, a plot of $1/k_{obsd}$ vs. $1/[OH^-]$ should be a straight line. Deviations from the equilibrium assumption would result if $k_i \gg k_{-1}$, a condition that is independent of pH, or if $k_1[OH^-] \ll k_i$, a condition that is certain to result in departures from equilibrium when the pH is low.

In Figure 6 the solid line represents a calculated curve predicted by equation 6 with rate constants derived from the 10 experimental rate constants for pHs between 10.35 and 12.90 [$k_i = (2.3 \pm 0.3) \times 10^{-3}$ min^{-1}, $K = 674 \pm 34$, $r^2 = 0.997$). The excellent fit between pH 10 and pH 12 is obvious, as is the lack of fit at higher pHs. At pH 9.7, the deviation is thought to be the result of the failure of the equilibrium assumption (see above).

Although this pathway is intuitively attractive, it alone does not explain the rate behavior at pHs above 12. Clearly, some other unknown processes are operative at higher pHs. The behavior here, although it gives a linear log k vs. pH plot, is still *not* first order in hydroxide activity.

Additional support for the existence of a charge intermediate is provided by the results of studies in mixed solvents. Both our data and those of other investigators are tabulated in Tables II and III and shown graphically in Figure 3. The pseudo-first-order rate constants at constant pH in methanol–water decrase linearly as the volume percent methanol is increased up to 50% (Table II). In acetonitrile–water the same behavior is observed except that the rate of decrease is more pronounced.

In the log k vs. pH plots shown in Figures 3, 6, and 7, two points should be noted. First, the linear portion (slopes) of the plots are similar. Second, the linear portion extends about 1 pH unit lower for 50% methanol than for water. For 50% acetonitrile, only a linear plot was obtained over the pH range investigated.

These solvent effects are consistent with the existence of the pentavalent intermediate shown in equation 4. It is well documented that a non-protic solvent does not effectively stabilize an anionic intermediate through hydrogen bonding as do the protic solvents water and methanol (Hammett, 1970). Therefore, the behavior in acetonitrile is not consistent with eq 6. Rather, the kinetics are more similar to the high pH behavior in water and methanol–water.

In the case of methanol, the reason for the increase in the magnitude of the equilibrium constant (in eq 6) relative to water is not as obvious. It is generally recognized, however, that for solutions of dielectric constants greater than 30, the kinetic effect of increasing the dielectric constant is minor relative to specific solvation effects.

The observation of pronounced solvent effects, therefore, is to be expected in reactions involving an anionic intermediate. This can be contrasted to the alternative mechanism involving hydroxide attack on phosphorus as the rate-limiting step, which would be expected to result in less pronounced solvent effects.

CONCLUSIONS

Chlorpyrifos undergoes a pH-independent hydrolysis reaction over the environmentally relevant pH range of 4–7.5 with a first-order disappearance rate constant of $(6.2 \pm 0.9) \times 10^{-6}$ min^{-1} (half-life, 78 days) at 25 °C. Above pH 8, alkaline hydrolysis dominates, but the reaction does not obey second-order kinetics. The kinetics are consistent, however, with the formation of an anionic intermediate over the pH range of 9–12. Above pH 12, another unidentified reaction, also non first order in hydroxide, is operative but results in the same major products as are formed at the lower pHs. Thus, extrapolation of alkaline hydrolysis rate constants obtained at a single pH to other pHs should be viewed with caution. To confirm this tentative mechanism involving an anionic intermediate, direct evidence is required and experiments to obtain such evidence are being pursued. Also, other organophosphorothioate esters should be investigated to deter-

mine whether this is a general mechanism.

ACKNOWLEDGMENT

We thank Alfred Thruston, Analytical Chemistry Branch, Environmental Research Laboratory, Athens GA, for providing LC–MS data. Also, we thank Dennis Revell and Myron Stephenson, Environmental Services Division, Region IV, U.S. Environmental Protection Agency, Athens, GA, for providing GLC–MS data. Our thanks also to Rudolph Parrish, Computer Science Corp., Athens, GA, for help with the mathematical modeling. We are also indebted to Patricia Schlotzhauer of the Athens Laboratory for her assistance in carrying out parts of the experimental work.

Registry No. Chlorpyrifos, 2921-88-2; 3,5,6-trichloro-2-pyridinol, 6515-38-4; *O,O*-diethyl phosphorothioic acid, 2465-65-8.

LITERATURE CITED

Barnard, P. W. C.; Bunton, C. A.; Llewellyn, D. R.; Vernon, C. A.; Welch, V. A. *J. Chem. Soc.* **1961**, 2670.
Bates, R. G. "Determination of pH: Theory and Practice"; Wiley: New York, 1964.
Brust, H. F. *Down Earth* **1966**, 21.
Bunnett, J. F. In "Technique of Organic Chemistry VIII. Rates and Mechanisms of Reactions, Part I"; Friess, S. L.; Lewis, E. S.; Weissberger, A., Eds.; Interscience: New York, 1961; p 177.
Cox, J. R., Jr.; Ramsay, B. *Chem. Rev.* **1964**, *64*, 317.
"Farm Chemicals Handbook" Farm Chemicals, Meister Publishing Co.: Willoughby, OH, 1981.
Freed, V. H.; Schmedding, D.; Kohnert, R.; Haque, R. *Pestic. Biochem. Physiol.* **1979**, *10*, 203.
Frost, A. A.; Pearson, R. G. "Kinetics and Mechanism", 2nd ed.; Wiley: New York, 1961; p 150.
Hammett, L. P. "Physical Organic Chemistry", 2nd ed.; McGraw-Hill: New York, 1970.
Macalady, D. L.; Wolfe, N. L., submitted for publication in *Environ. Sci. Technol.*, 1983.
Meikle, R. W.; Youngson, C. R. *Arch. Environ. Contam. Toxicol.* **1978**, *7*, 13.
Paris, D. F.; Steen, W. C.; Baughman, G. L.; Barnett, J. T., Jr. *Appl. Environ. Microbiol.* **1981**, *41*, 603.
Perdue, E. M.; Wolfe, N. L. *Environ. Sci. Technol.* **1983**, in press.
Smith, J. H.; Mabey, W. R.; Bohonos, N.; Holt, B. R.; Lee, S. S.; Chou, T. W.; Bomberger, D. C.; Mill, T. "Environmental Pathways of Selected Chemicals in Freshwater Systems: Part II. Laboratory Studies"; U.S. Environmental Protection Agency: Athens, GA, 1978; EPA-600/7-78-074.
Webb, R. C.; Garrison, A. W.; Keith, L. H.; McGuire, J. M. "Current Practice in GC-MS Analysis of Organics in Water"; U.S. Environmental Protection Agency: Athens, GA, 1973; EPA-R2-73-277.
Weber, K. *Water Res.* **1976**, *10*, 237.
Wolfe, N. L. *Chemosphere* **1980**, *9*, 571.
Wolfe, N. L.; Paris, D. F.; Steen, W. C.; Baughman, G. L. *Environ. Sci. Technol.* **1980**, *14*, 1143.
Wolfe, N. L.; Zepp, R. G.; Paris, D. F. *Water Res.* **1978**, *12*, 565.
Younas, M. *Pak. J. Sci.* **1972**, *24*, 100.

Received for review November 30, 1982. Revised manuscript received May 26, 1983. Accepted July 6, 1983. Mention of trade names or commercial products does not constitute endorsement or recommendation for use by the U.S. Environmental Protection Agency.

Determination of the Phenolic Metabolites of Carbofuran in Plants by Gas Chromatography/Mass Spectrometry

Thomas R. Nelsen,*[1] Ronald F. Cook, Michael H. Gruenauer, Mason D. Gilbert, and Sujit Witkonton

A gas chromatographic procedure using mass spectrometry in the selected ion mode as the detection system for the determination of residues of the phenolic metabolites of carbofuran (2,3-dihydro-2,2-dimethyl-7-benzofuranyl methylcarbamate) is described. The method is general, having been applied without change to 12 different crop matrices including those having high-moisture, low-moisture, and high-lipid content, as well as fruit, vegetable, and root crops. Method sensitivities of 0.05–0.10 ppm for each phenol were achieved. Average recoveries of the three phenolic metabolites ranged from 72 to 104%. The method involved release of the conjugated phenols by acid hydrolysis, extraction, ethoxylation, partition of the phenols into base, acidification, extraction, and silica gel Sep-PAK cleanup of the samples.

Investigations by Metcalf et al. (1968) and Knaak et al. (1970a,b) have shown that there are three major phenolic metabolites of carbofuran (2,3-dihydro-2,2-dimethyl-7-benzofuranyl methylcarbamate). These metabolites were identified as 2,3-dihydro-2,2-dimethyl-7-benzofuranol (7-phenol), 2,3-dihydro-2,2-dimethyl-3-oxo-7-benzofuranol (3-keto-7-phenol), and 2,3-dihydro-2,2-dimethyl-3,7-benzofurandiol (3-hydroxy-7-phenol). The phenolic residues occur as water-soluble conjugates bound at the 3- and/or 7-position of the benzofuranol system.

Only one residue procedure of any generality has been reported for these phenols (Cook et al., 1977). This method detected the phenols as their dinitrophenyl ether derivatives. Archer et al. (1977) have reported a similar residue method for these compounds in strawberry and strawberry leaves. The general procedure reported by Cook is workable; however, the procedure is a lengthy, complex, multistep procedure. The chromatographic cleanup of the samples is variable from crop matrix to crop matrix and low-level coextractive interferences created quantitation

FMC Corporation, Agricultural Chemicals Group, Princeton, New Jersey 08540.
[1]Present address: Diamond Shamrock Corp., T. R. Evans Research Center, Painesville, OH 44077.

0021-8561/83/1431-1147$01.50/0